Chapter 16
Radio Frequency Interference

A basic requirement of radio astronomy is access to a spectrum in which observations can be made without detrimental interference from transmissions by other services. In the early years of radio astronomy, when most of the radio astronomy bands below a few GHz were allocated, bandwidths of radio astronomy systems were generally no greater than a few MHz, and the comparable allocated bandwidths largely sufficed. Some allocations were made for radio lines, most importantly the hydrogen (H1) line, for which 1420–1427 MHz was reserved. In the following decades, as radio astronomy at frequencies in the range of tens of GHz developed, bandwidths of order 1 GHz were allocated, and later, a substantial fraction of the spectrum above $\sim$ 100 GHz was allocated to radio astronomy. However, spillover of radiation from transmitting services into radio astronomy bands occurs, and generally it has been necessary to choose observatory sites in radio-quiet areas of low population density and to take advantage of terrain shielding where possible. These considerations have led to the choice of sites in South Africa and Western Australia for international development of several of the largest arrays. Also, with the increase in computing capacity at observatories, detection and removal of interfering signals in astronomical observations have become important parts of data analysis. In particular, digital analysis allows the received bandwidths to be divided into as many as 10^6 spectral channels, which allows those containing interference to be identified and removed. A general discussion of interference in radio astronomy is given by Baan (2010).

The most serious interference usually results from intentional radio radiation such as those used for transmission of information in many forms, or for radio location, etc. Interference can also occur as a result of unintentional emissions from electrical machinery and industrial processes such as welding. Such emissions often take the form of trains of short electromagnetic pulses. For example, a rectangular

A.R. Thompson, J.M. Moran, and G.W. Swenson Jr., *Interferometry and Synthesis in Radio Astronomy*, Astronomy and Astrophysics Library,
DOI 10.1007/978-3-319-44431-4_16

pulse of width δt has a power spectrum

$$P(\nu) \sim \left[\frac{\sin \pi \nu \delta t}{\pi \nu \delta t}\right]^2 . \tag{16.1}$$

Most of the power is contained in the frequency range between DC and $1/\delta t$. However, the envelope of the power spectrum decreases only as ν^{-2}, and hence, such interference can be a problem at frequencies much higher than $1/\delta t$. Electromagnetic interference (EMI) of this type is usually most serious at frequencies below a few GHz. A detailed analysis of radiation produced by sparks in power lines was developed by Beasley (1970). To avoid such interference, sites for radio astronomy observatories are located in relatively undeveloped areas, and proximity to industries and major highways is avoided. Necessary vehicles and machinery on observatory sites are generally fitted with filtering components that strongly reduce unwanted emissions. Shielding of electronic equipment is very important.

16.1 Detection of Interference

A basic problem is the identification of the contaminated data. In the simplest case, this is a matter of examining the output of a correlator or detector and deleting data in which the signal amplitude is larger than expected or does not vary with time or antenna pointing in the manner expected for astronomical sources. In earlier times, interference removal sometimes meant losing the whole bandwidth received, but as mentioned above, use of multichannel spectral processing permits deletion of only the contaminated channels. The greatest difficulty is the detection of weak interference. Use of channel bandwidths comparable to the bandwidth of an interfering transmitter also has the advantage of maximizing the interference-to-noise ratio, thus improving the detectability.

When inspecting data for variations that indicate the presence of interference, data averaging times of seconds or minutes are often appropriate when the interference varies on similar timescales. However, the astronomical measurements may require averaging of data over periods of many hours to obtain the required sensitivity, so interference at levels that can introduce errors in the data may be too weak relative to the noise to be easily detected. With the high data output rates produced by large synthesis arrays, it is impractical to examine all of the data manually, and algorithms by which contaminated data can be flagged by computer are important. Methods of dealing with radio interference include (1) those that simply delete receiver output data that are believed to be contaminated by interference; (2) those that cancel or reduce the interference without removing the astronomical data that occur at the same time and frequency; and (3) those that involve spatial filtering, in which a null is generated in the antenna reception pattern in the direction of an interferer.

The common characteristic of interfering signals is that, in general, their sources do not move relative to the antennas at the sidereal rates of astronomical objects.

When the effects of the sidereal motion of the astronomical target are removed from the correlated data, the fringe frequency variations are transferred to any extraneous signals, and thus the unwanted signals can be identified by the fringe rate variations in their phases. For long baselines where the fringe rates are high, the interference will be attenuated by the subsequent time averaging of the data (e.g., Perley 2002). However, in many cases, some further analysis is required to remove the effects of the interference, as considered in Sect. 16.2. Athreya (2009) describes the application to the Giant Metrewave Radio Telescope array in India.

Some examples of techniques to detect the presence of interference are as follows. For a general overview, see also Fridman and Baan (2001), Briggs and Kocz (2005), and Baan (2010).

1. Use of monitoring receivers with antennas pointed toward likely sources of interference, such as toward the horizon for terrestrial transmitters (e.g., Rogers et al. 2005).
2. Comparison of data taken simultaneously at two observatories that are sufficiently widely separated that interference from any transmitter is unlikely to be received at both. This has been used in the search for pulses and other transient astronomical emissions (e.g., Bhat et al. 2005).
3. Detection of transmissions with cyclostationary characteristics, that is, transmission in which some characteristic repeats at intervals τ_c in time. Examples are the frame cycles in TV signals and repeated data cycles in GPS (global positioning system) transmissions. Values of τ_c can be determined for the expected signal environment. The occurrence of components of the data with cyclostationary characteristics can be investigated by performing an autocorrelation and looking for features that repeat at intervals τ_c. Bretteil and Weber (2005) find that searching for a Fourier component at frequency $1/\tau_c$ in the data is an advantageous method.
4. Use of the closure amplitude relationships [Eq. (10.44)] can provide an indication of interference. If observations are made of a point source in the absence of interference, the visibility ratios on the right side of the equation are equal to unity, and the values of r_{ij} on the left side are proportional to the corresponding main-beam gains. A signal from an interfering source will add a component to the output, the magnitude of which will depend upon the sidelobe gains of the antennas, which will vary with time as the antennas track. Thus, variation of the closure gain values is an indication of possible interference. Note, however, that the correction for the fringe frequency of the target source will cause variation of the same frequency in the response to interference from a stationary transmitter, so the effect of the interference will decrease (i.e., the interference threshold will increase) with an increase of the baseline component u, as discussed in Sect. 16.3.2.
5. In the case of interference from radar pulses, the individual pulses are sometimes strong enough to be seen by looking at the output of a detector, especially if the transmitter is close enough that a direct signal path exists. It may be possible to determine the timing pattern of the pulses and generate blanking pulses for the radio astronomy receivers. The situation may be such that it is necessary to

extend the blanking to include reflections from nearby aircraft, etc. See, e.g., the discussion by Dong et al. (2005). A buffer memory for the data allows blanking to begin just before the pulse is detected, to ensure effective removal.

6. An interesting object lesson is the identification of solitary radio bursts of millisecond duration with swept frequency vs. time characteristics similar to those of pulsars. These events were known as perytons. The radiation entered multiple channels of the telescope's multibeam receivers, showed peculiar kinks in the time frequency dependence, and preferentially occurred at midmorning. These characteristics led to the source: prematurely opened doors of microwave ovens at the observatory (Petroff et al. 2015).
7. Examination of the statistics of the receiver output data. Kurtosis is defined as μ_4/μ_2^2, where μ_2 and μ_4 are the mean values of the second and fourth powers of the data with respect to the mean value. For Gaussian noise, kurtosis has a value of 3.0, and other values are an indication of non-Gaussian data (Nita et al. 2007; Nita and Gary 2010).
8. With high-resolution multichannel receivers, interference can be detected and excised from deviant channels (e.g., Leshem et al. 2000).

16.1.1 Low-Frequency Radio Environment

The LOw Frequency ARray (LOFAR array; see Sect. 5.7.1), which is located in the Netherlands with long baseline extensions in other countries, covers the frequency ranges 10–80 and 110–240 MHz, thus avoiding the FM broadcast band. Discussions of the problem of radio interference in these frequency ranges are given by Boonstra and van der Tol (2005) and Offringa et al. (2013). The latter provides a detailed examination of the radio environment in the 30–78 MHz and 115–163 MHz ranges. For these measurements, the received signals were split into 512 sub-bands of 195 kHz width. The spectral resolution of the data was 0.76 kHz. Offringa et al. (2013) found that the interference occupancy was 1.8% for the lower band and 3.2% for the higher one. They concluded that these levels of narrowband interference should not significantly restrict astronomical observations, but that it is important that the frequency range of LOFAR remain free of broadband interference. A similar analysis has been carried out for the Murchison Widefield Array in Western Australia (Offringa et al. 2015).

16.2 Removal of Interference

When possible, mitigation of interference by cancellation, leaving the astronomical data intact, is clearly preferable to total deletion of the corrupted data. Cancellation requires not only detection but also an accurate estimation of the interfering signal in order to remove it. In *adaptive* cancellation [see, e.g., Barnbaum and Bradley (1998)], a separate antenna (usually smaller than the astronomy antenna) is pointed toward the interferer. The received signal from this antenna is digitized, passed

through an adaptive filter, and combined with the signal from the astronomy antenna. The combined outputs are processed by an algorithm that provides a control of the adaptive filter in such a way as to cause the interfering signal voltages from the two antennas to cancel each other. Of various algorithms that could be used to control the adaptive filter, Barnbaum and Bradley used a least-mean-squares algorithm, which is computationally simple and thus easily adapted to follow the relative variation of the astronomical and interfering signals as the astronomy antenna tracks. All of this takes place before the signals reach the correlator or detector. Briggs and Kocz (2005) give an example of an interference cancellation scheme in which the outputs of the astronomy and interference antennas are cross-correlated to provide a control for the adaptive filter. For a detailed discussion of methods involving cross-correlation of astronomy antenna outputs with those of axillary antennas directed toward the source of interference, see Briggs et al. (2000). In some cases in which the structure of the interfering signal is known in detail, as in the case of the GLONASS (Global Navigation Satellite System) navigational satellite signals, it is possible to recreate the interfering signal from the interference received in the astronomy antenna with sufficient accuracy for cancellation. In an example discussed by Ellingson et al. (2001), interference from GLONASS was reduced by 20 dB.

16.2.1 Nulling for Attenuation of Interfering Signals

Spatial nulling involves using a group of antennas in which a null in the combined spatial response is formed in the direction of the source of interference. In low-frequency arrays in which the individual receiving elements are dipoles with beams covering much of the sky, such nulling may also result in loss of astronomical sky coverage.

In *deterministic* nulling, the direction of the interferer is known, and a null is formed in that direction by weighting the signals received. Weighting factors (in amplitude and phase) can be applied to the signals from individual antennas if they are being combined, as in a phased array, or to the correlated products from antenna pairs before they are combined to form an image. It is not necessary to be able to identify the interference within the received signal, but if the angular responses in the direction of the null differ from one antenna to another, it is necessary to calibrate the antenna responses, which may not be practicable for the far sidelobes. Deterministic nulling can be applied to a synthesis array in two ways. First, the nulls can be formed by adjusting the weights with which the cross products of the outputs of pairs of antennas (the visibility values) are combined. In this case, the nulls are formed in the synthesized beam pattern, i.e., most likely in the sidelobes of the synthesized beam unless the direction of the interferer is within the synthesized field. Second, in the case of synthesis arrays in which the elements between which cross-correlations are formed are themselves phased subarrays of antennas, the nulls can be formed in the subarray beams. In this case, the weighting is applied directly to the signals from the individual antennas.

16.2.2 Further Considerations of Deterministic Nulling

Consider an array of n nominally identical antennas, each of which is connected through a phase shifter to an n-to-1 power combiner. Each picks up a power level p from an interfering signal. In the power combiner, the power is divided n ways between the other antennas and the output. Thus, each antenna contributes a power level p/n to the combiner output. The voltage contributions of the antennas can be represented by vectors of amplitude $\sqrt{p/n}$. If the phase shifters are adjusted so that the contributions combine in phase, the vectors are aligned and the output voltage is $\sqrt{np}$. The output power is np, as expected, since the total collecting area is n times that of a single antenna. Now suppose that the phase shifters are set so that the signal vectors combine with random phase angles. The combined voltage has an expectation of $\sqrt{n}$ times that of a single antenna. Thus, the expectation of the combined power received is equal to that from a single antenna, p (see Sect. 9.9 for a related discussion of phasing of arrays). Finally, consider the case in which the phases are adjusted so that the vectors form a closed loop with zero resultant, thus producing a null in the direction of incidence of the signal. If each signal vector has a random error in amplitude and phase of relative rms amplitude ϵ, then the vector sum will fail to close by an amount equal to the sum of the errors, i.e., $\sim \epsilon\sqrt{p}$, resulting in a power level of $\epsilon^2 p$. Thus, a null of depth x dB below the response of a single antenna requires $\epsilon = 10^{-x/20}$, e.g., $\epsilon = 0.03$ for a null depth of 30 dB. These requirements on the accuracy of the voltage responses apply to the interference components identified in adaptive nulling and to the accuracy of the antenna responses in deterministic nulling. In closing the vector loop for a null, the shape of the loop is not constrained, so free parameters remain for forming beams or nulls in other directions.

In forming a null in a given direction, one can start by determining the complex gain factors required to close the vector loop on the assumption that the antennas are all ideal isotropic radiators. Then, to take account of the actual gain of the antennas, each signal vector has to be multiplied by a further complex gain factor. If this second gain factor is the same for each antenna, the size and orientation of the vector loop may be changed, but it will remain closed. Thus, the response factor in the direction of the interferer need not be known so long as it is identical for all antennas. If the gain factor differs from one antenna to another, as is likely to be the case for signals received through far sidelobes, the loop will not close unless the individual gain factors are known and taken into account. The need to calibrate the far sidelobes of a high-gain reflector antenna over a large fraction of 4π steradians, and perhaps also as a function of frequency across receiver bandwidth, limits the usefulness of deterministic nulling in such cases. Deterministic nulling is discussed by Smolders and Hampson (2002); Ellingson and Hampson (2002); Ellingson and Cazemier (2003); Raza et al. (2002); and van der Tol and van der Veen (2005).

16.2.3 Adaptive Nulling in the Synthesized Beam

A way of removing the effects of an interfering signal is to place a null in the reception pattern of an array of antennas in the direction of incidence of the interference. This can be done in software and is referred to as adaptive nulling. In general, the direction of incidence of the interference is not known and must be deduced from the observations. Adaptive nulling, in which the system reacts automatically to an interfering signal, generally requires that the interference is not too strong and originates from a single source. It can also result in a significant computing load. Details can be found in Leshem and van der Veen (2000); Ellingson and Hampson (2002); Raza et al. (2002); and van der Tol and van der Veen (2005).

16.3 Estimation of Harmful Thresholds

In the efforts to obtain protection for radio astronomy observations in the systems of frequency regulation within the International Telecommunication Union (ITU), and also within the regulatory systems of individual nations, it has been essential for radio astronomers to provide quantitative estimates of the threshold levels of signal power that are harmful to astronomical observations. These vary with frequency and also with the type of radio telescopes involved. This section is concerned with the estimation of these harmful thresholds, particularly for the frequency bands allocated to radio astronomy.

The ultimate limit on the sensitivity of a radio telescope is set by the system noise, and an interfering signal can generally be tolerated if its contribution to the output image is small compared with the noise fluctuations. A response to interference of one-tenth of the rms level of the noise in the measurements is a useful criterion in interference threshold calculations. The corresponding flux density of such a signal can be calculated if the effective collecting area of the antenna, in the direction of the interference, is known. Except at the longer wavelengths, radio astronomy antennas usually have narrow beams, and the probability of the interfering signal being received in the main beam or nearby sidelobes is low, especially if the interfering transmitter is ground based. Thus, we assume here that interference usually enters the far sidelobes of the antenna. Figure 16.1 shows an empirical model curve for the maximum sidelobe gain as a function of angle from the main-beam axis. This curve is derived from the measured response patterns of a number of large reflector antennas. For the present estimate, it is appropriate to use a gain of 0 dBi (i.e., 0 dB with respect to an isotropic radiator), which occurs at about 19° from the main beam. Zero dBi is also the mean gain of an antenna over 4π steradians, and the effective collecting area for this gain is equal to $\lambda^2/4\pi$, where λ is the wavelength. If F_h (W m^{-2}) is the flux density of an interfering signal within the receiver passband, the

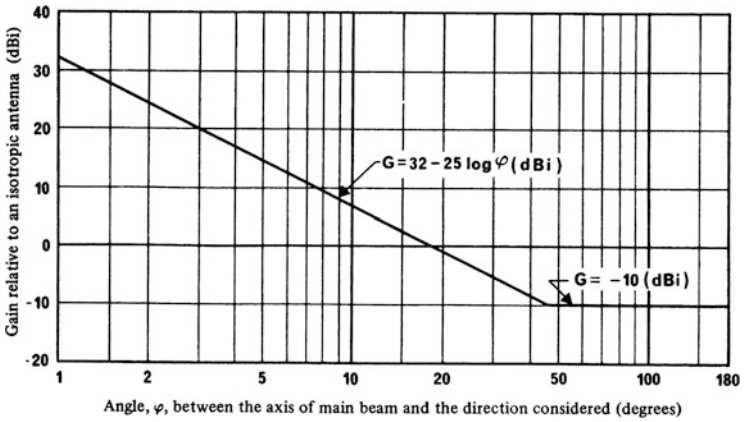

Fig. 16.1 Empirical sidelobe-envelope model for reflector antennas of diameter greater than 100 wavelengths. Measurements on antennas show that 90% of sidelobe peaks lie below the curve. Sidelobe levels can be reduced by 3 dB or more in designs in which aperture blockage by feed structure is eliminated or minimized. The model shown is representative of large antennas with tripod or quadrupod feed supports of the type commonly used in radio astronomy. From ITU-R Recommendation SA.509-1 (1997).

interference-to-noise power ratio in the receiver is

$$\frac{F_h \lambda^2}{4\pi k T_S \Delta\nu} , \tag{16.2}$$

where k is Boltzmann's constant, T_S is the system noise temperature, and $\Delta\nu$ is the receiver bandwidth. In this expression, it is assumed that the polarization of the interfering signal matches that of the antenna. Since radio astronomy antennas commonly receive two polarizations, crossed linear or opposite circular, choice of antenna polarization is of little help in avoiding interference. In practice, the received level of the interfering signal varies with time because of propagation effects and the tracking motion of the radio telescope, which sweeps the sidelobe pattern across the direction of the transmitter.

For comparison with correlator systems, we first consider the simpler case of a receiver that measures the total power at the output of a single antenna. The interference-to-noise ratio of the output, after square-law detection and averaging for a time τ_a, is expression (16.2) multiplied by $\sqrt{\Delta\nu\tau_a}$. This result follows from considerations similar to those discussed in Sect. 6.2.1. Then for an output interference-to-noise ratio of 0.1, which we use as the criterion for the threshold of harmful interference,

$$F_h = \frac{0.4\pi k T_S \nu^2 \sqrt{\Delta\nu}}{c^2 \sqrt{\tau_a}} . \tag{16.3}$$

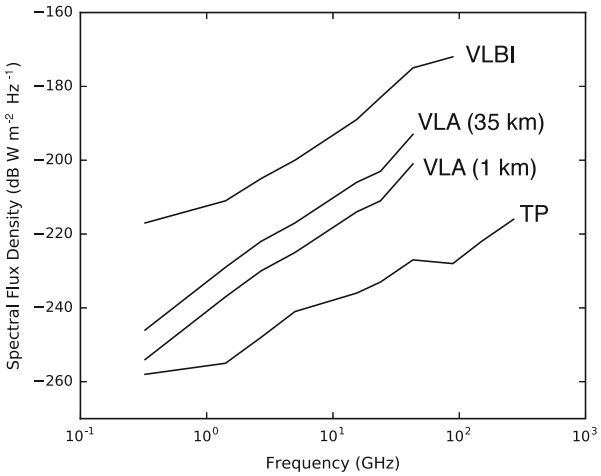

Fig. 16.2 Curves of the estimated harmful threshold of interference in dBW m^{-2} Hz^{-1}. The lowest curve is for total power (TP) measurement on a single antenna, and the topmost curve is for VLBI. The data in these are from ITU-R Recommendation RA.769-2 (2003) and essentially represent the considerations in Sects. 16.3 and 16.5. The smaller variations result from the characteristics of individual instruments. The two middle curves in the figure represent synthesis arrays and are based on the VLA at the most compact and most extended configurations, for which the corresponding spacings vary by a factor of about 35. The major feature in all of the curves is the increase with frequency, which results mainly from the effective collecting area of the receiving sidelobes, which varies as ν^{-2}. Because of various simplifying assumptions, the results in this figure are only approximate but also provide an indication of the relative vulnerability of different types of observations.

Note that the harmful threshold increases with frequency as ν^2 as a result of the dependence of the sidelobe collecting area. With increasing frequency, the system temperature and the usable bandwidth also generally increase. Expressed in spectral power flux density, the corresponding threshold level, S_h (W m^{-2} Hz^{-1}), is

$$S_h = \frac{F_h}{\Delta\nu} = \frac{0.4\pi k T_S \nu^2}{c^2\sqrt{\tau_a\,\Delta\nu}}\,. \tag{16.4}$$

To determine the harmful interference level for continuum observations within a band allocated to radio astronomy, $\Delta\nu$ is usually taken to be the width of the allocated band. The total-power type of radio telescope is the most sensitive to interference. Thus, the results in Eqs. (16.3) and (16.4) provide a worst-case specification for the harmful thresholds of interference for radio astronomy. Values of F_h and S_h computed for total-power systems using typical parameters for the various radio astronomy bands are given in ITU-R[1] documentation (ITU-R 2013). For S_h, the values are plotted as the bottom curve in Fig. 16.2. Since much of the

[1]ITU-R denotes the Radiocommunication Sector of the International Telecommunication Union.

interference to radio astronomy results from broadband spurious emissions, S_h is particularly useful.

Low-level interference, of amplitude comparable to the noise in the receiver output, degrades the sensitivity and impedes the ability to detect weak sources. Thus, in observations in which interference has occurred, it is often necessary to delete any data that appear to be corrupted. The analysis that follows considers the response to interference resulting from basic methods of observation and data reduction and does not include procedures designed specifically for mitigation of interference.

16.3.1 Short- and Intermediate-Baseline Arrays

We now consider the interference response of a correlator array with antenna spacings from a few meters to a few tens of kilometers. Two effects reduce the response to interference compared with that of a total-power system. First, the source of interference does not move across the sky with the sidereal motion of the object under observation, and thus it produces fringe oscillations of a different frequency from those of the wanted signal. Second, the instrumental delays are adjusted to equalize the signal paths for radiation incident from the direction of observation, and signals from another direction, if they are broadband, are to some extent decorrelated. The following analysis is based on Thompson (1982).

16.3.2 Fringe-Frequency Averaging

Consider first the fringe-frequency effect. Suppose that instrumental phase shifts are introduced, as described in Sect. 6.1.6, to slow the fringe oscillations of the wanted signal to zero frequency. The removal of the fringe-frequency phase shifts from the cosmic signals introduces corresponding shifts into the interfering signals. If the source of interference is stationary with respect to the antennas, the interference at the correlator output has the form of oscillations at the natural fringe frequency for the source under observation, which from Eq. (4.9) (omitting the sign of dw/dt) is

$$\nu_f = \omega_e u \cos\delta \ . \tag{16.5}$$

Here ω_e is the angular rotation velocity of the Earth, u is a component of antenna spacing, and δ is the declination of the source under observation. Averaging of such a fringe-frequency waveform for a period τ_a is equivalent to convolution with a rectangular function of width τ_a. The amplitude is thus decreased by a factor that follows from the Fourier transform of the convolving function. This factor is

$$f_1 = \frac{\sin(\pi \nu_f \tau_a)}{\pi \nu_f \tau_a} \ . \tag{16.6}$$

In order to estimate a harmful threshold for interference (F_h), we compute the ratio of the rms level of interference to the rms level of noise in a radio image and, as before, equate the result to 0.1. The first step is to determine the mean squared value of the modulus of the interference component in the visibility data. Figure 6.7b, which depicts the spectral components at the correlator output, shows that the output from the correlated signal component, in this case the interference, is represented by a delta function. Assuming, as before, that the interference enters sidelobes of gain 0 dBi and that the polarization is matched, we substitute in the magnitude of the delta function $kT_A\,\Delta\nu = F_h c^2/4\pi\nu^2$. Thus, the sum of the squared modulus of the interference over n_r grid points in the (u, v) plane is

$$\sum_{n_r} \langle |r_i|^2 \rangle = \left(\frac{H_0^2 F_h c^2}{4\pi\nu^2} \right) n_r \langle f_1^2 \rangle \ . \tag{16.7}$$

Here r_i is the correlator response to the interference, H_0 is a voltage gain factor, and $\langle f_1^2 \rangle$ is the mean squared value of f_1, as given in Eq. (16.6), which represents the effect of the visibility averaging on the fringe-frequency oscillations. To determine the mean squared value of f_1, a simple approach is to consider the variation of this factor in the (u', v') plane in which the antenna-spacing vector rotates with constant angular velocity ω_e and sweeps out a circular locus, as described in Sect. 4.2. Also, suppose that to interpolate the values of visibility at the rectangular grid points in the (u, v) plane, the measured values are averaged with uniform weight within rectangular cells centered on the grid points (see the description of cell averaging in Sect. 5.2.2). Then the effective averaging time τ for the interference is equal to the time taken by the baseline vector to cross a cell, as shown in Fig. 16.3. Note from Eq. (16.5) that the fringe frequency goes through zero at the v' axis, and f_1 is then unity. For small values of ψ, as defined in Fig. 16.3, the path length through a cell is closely equal to Δu, and the cell crossing time is $\tau = \Delta u/\omega_e q'$, where $q' = \sqrt{X_\lambda^2 + Y_\lambda^2}$, and where X_λ and Y_λ are the components of antenna spacing measured in wavelengths and projected onto the equatorial plane, as defined in Sect. 4.1. Also, $\nu_f \tau = \Delta u \sin\psi \cos\delta$. Now Δu is equal to the reciprocal of the width of the synthesized field, which, except at long wavelengths, is unlikely to be more than $\sim 0.5°$. We therefore assume that Δu is of order 100 or greater, which permits the following simplification. For $\Delta u = 100$ and $\delta < 70°$, f_1^2 goes from 1 to 10^{-3} as ψ goes from 0 to $< 17°$. Thus, most of the contribution to f_1^2 occurs for small ψ, and we can substitute $\nu_f \tau = \psi \Delta u \cos\delta$ in Eq. (16.6) and obtain

$$\langle f_1^2 \rangle = \frac{2}{\pi} \int_0^{\pi/2} \frac{\sin^2(\pi\psi\Delta u \cos\delta)}{(\pi\psi\Delta u \cos\delta)^2} d\psi \simeq \frac{1}{\pi \Delta u \cos\delta} \ . \tag{16.8}$$

Since Δu is large, we have used an upper limit of ∞ in evaluating the integral.

For the noise, we again refer to Fig. 6.7b. The power spectral density of the noise near zero frequency is $H_0^4 k^2 T_S^2 \Delta\nu$, and an equivalent bandwidth τ^{-1}, including

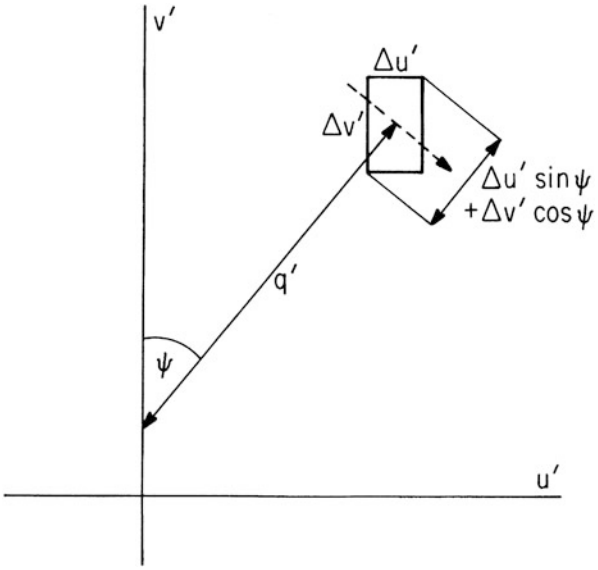

Fig. 16.3 Derivation of the mean cell crossing time for the spatial frequency locus indicated by the broken line. The velocity of the spatial frequency vector in the (u', v') plane is $\omega_e q'$. The mean path length through the cell in the direction of the broken line is the cell area $\Delta u' \Delta v'$ divided by the cell width projected normal to that direction.

negative frequencies, is passed by the averaging process; see Eq. (6.44). The mean-squared component of the noise over the n_r grid points is thus

$$\sum_{n_r} \langle |r_n| \rangle^2 = H_0^4 k^2 T_S^2 \Delta\nu n_r \langle \tau^{-1} \rangle \ , \tag{16.9}$$

where $\langle \tau^{-1} \rangle$ is the mean value of τ^{-1}. From Fig. 16.3, the mean cell crossing time is

$$\tau = \frac{\Delta u \, |\mathrm{cosec}\, \delta|}{q' \omega_e \, (|\sin \psi| + |\mathrm{cosec}\, \delta| \, |\cos \psi|)} \ . \tag{16.10}$$

We have assumed that $\Delta u' = \Delta v' \sin \delta$ (i.e., $\Delta u = \Delta v$) and that for all except a small number of cells, the path of the spatial frequency locus through a cell can be approximated by a straight line. The mean value of τ^{-1} around a locus in the (u', v') plane (see Sect. 4.2) is, from Eq. (16.10),

$$\frac{2}{\pi} \int_0^{\pi/2} \tau^{-1} d\psi = \frac{2\omega_e q'}{\pi \Delta u} (1 + |\sin \delta|) \ , \tag{16.11}$$

and the mean for the n_r points in the (u, v) plane is

$$\left\langle \tau^{-1} \right\rangle = \frac{2\omega_e}{\pi \Delta u} (1 + |\sin\delta|) \frac{1}{n_r} \sum_{n_r} q' \,. \tag{16.12}$$

From Eqs. (16.7)–(16.9) and Eq. (16.12), the interference-to-noise ratio is

$$\frac{(|r_i|)_{\text{rms}}}{(|r_n|)_{\text{rms}}} = \frac{F_h c^2}{4\pi k T_S \nu^2 \sqrt{2\Delta\nu\omega_e \cos\delta (1 + |\sin\delta}} \frac{1}{\sqrt{\frac{1}{n_r}\sum_{n_r} q'}} \,. \tag{16.13}$$

By Parseval's theorem, the ratio of the rms values of the interference and noise in the image is equal to the same ratio in the visibility domain, which is given by Eq. (16.13). To evaluate the harmful threshold F_h, we equate the right side to 0.1 and obtain

$$F_h = \frac{0.4\pi k T_S \nu^2 \sqrt{2\Delta\nu\omega_e}}{c^2} \sqrt{\frac{1}{n_r} \sum_{n_r} q'} \,. \tag{16.14}$$

The factor $\sqrt{\cos\delta(1 + |\sin\delta}$ has been replaced by unity, the resulting error being less than 1 dB for $0 < |\delta| < 71°$, and 2.3 dB for $\delta = 80°$. The number of points in the (u', v') plane to which an antenna pair contributes is proportional to q', so in evaluating Eq. (16.14), it is convenient to write

$$\frac{1}{n_r} \sum_{n_r} q' = \frac{\sum_{n_p} q'^2}{\sum_{n_p} q'} \,, \tag{16.15}$$

where n_p is the number of correlated antenna pairs in the array.

The interference threshold S_h, in units of dBW m^{-2} Hz^{-1}, is given by

$$S_h = \frac{F_h}{\Delta\nu} = \frac{0.4\pi k T_S \nu^2 \sqrt{2\omega_e}}{c^2 \sqrt{\Delta\nu}} \sqrt{\frac{1}{n_r} \sum_{n_r} q'} \,. \tag{16.16}$$

Note that q' is proportional to ν, so S_h is proportional to $\nu^{2.5}$. Values of S_h for the VLA are shown by two middle curves in Fig. 16.2, which correspond to configurations in which the maximum baselines are 35 and 1 km, respectively (see Fig. 5.17b).

Since the averaging is ineffective in reducing the interference when u goes through zero, visibility values containing the greatest contributions from interference cluster around the v axis. Some degree of randomness in the occurrence of high values is to be expected, as a result of the varying sidelobe levels through which the interference enters. Because of the (u, v) distribution, the interference in the image domain takes the form of quasi-random structure that is elongated

in the east–west direction; for an example, see Thompson (1982). The clustering also suggests the possibility of reducing the interference response by deleting any questionable visibility data near the v axis. The resulting degradation of the (u, v) coverage would increase the sidelobes of the synthesized beam.

The discussion above applies to cases in which the observation is of sufficiently long duration that the (u, v) plane is well sampled, and in which the strength of the interfering signal remains approximately constant during this time. If only a fraction α of the (u, v) loci cross the v axis, then a factor of $\sqrt{\alpha}$ should be introduced into the denominators of Eqs. (16.14) and (16.16). Strong, sporadic interference can produce different responses from that considered above.

16.3.3 Decorrelation of Broadband Signals

Since interfering signals are usually incident from directions other than that of the desired radiation, their time delays to the correlator inputs are generally not equal. Broadband interfering signals are thereby decorrelated to some extent, which further reduces their response. The reduction is not amenable to a general-case analysis like that resulting from averaging of the fringe frequency, but it can be computed for each particular antenna configuration and position of the interfering source. For this reason, and the fact that only broadband signals are reduced, the effect has not been included in the threshold equations (16.14) and (16.16).

At any instant during an observation, let θ_s be the angle between a plane normal to the baseline for a pair of antennas and the direction of the source under observation. θ_s defines a circle on the celestial sphere for which the delays are equalized. Similarly, let θ_i be the corresponding angle for the source of interference. The delay difference for the interfering signals at the correlator is

$$\tau_d = \frac{D\,|\sin\theta_s - \sin\theta_i|}{c}\ , \tag{16.17}$$

where D is the baseline length. Expressions for θ_s and θ_i can be derived from Eq. (4.3), since $\sin\theta_s = w\lambda/D$, where w is the third spacing coordinate as shown in Fig. 3.2, and λ is the wavelength. Suppose that the received interfering signal has an effectively rectangular spectrum of width $\Delta\nu$ and center frequency ν_0, defined either by the signal itself or by the receiving passband. By the Wiener–Khinchin relation, the autocorrelation function of the signal is equal to

$$\frac{\sin(\pi\Delta\nu\tau_d)}{\pi\Delta\nu\tau_d}\cos(2\pi\nu_0\tau_d)\ . \tag{16.18}$$

Expression (16.18) represents the real output of a complex correlator as a function of the differential delay τ_d. The imaginary output is represented by a similar expression in which the cosine function is replaced by a sine. Thus, the decorrelation of the

modulus of the complex output for a delay τ_d is given by the factor

$$f_2 = \frac{\sin(\pi \Delta\nu \tau_d)}{\pi \Delta\nu \tau_d} \,. \tag{16.19}$$

For a fixed transmitter location, θ_i remains constant, but θ_s varies as the antennas track. Thus, τ_d may go through zero, causing f_2 to peak, but unlike f_1 in Eq. (16.6), a peak in f_2 can occur at any point on the (u, v) plane. Those antenna pairs for which the f_1 and f_2 peaks overlap contribute most strongly to the interference in the image, and those for which the peaks are well separated contribute less. Therefore, for broadband signals, the fringe-frequency and decorrelation effects should be considered in combination. For example, in calculations for the response of the VLA to a geostationary satellite on the meridian, a factor

$$\sqrt{\frac{\sum q' f_1^2 f_2^2}{\sum q' f_1^2}} \tag{16.20}$$

was computed that represents the additional decrease in the rms interference resulting from decorrelation (Thompson 1982). The summations in (16.20) were taken over all antenna pairs for equal increments in hour angle, and the q' factors were inserted to compensate for the uneven density of the sampled points in the (u, v) plane. The antenna spacings of the VLA for both the most compact and most extended configurations were considered, with observing frequencies from 1.4 to 23 GHz and bandwidths of 25 and 50 MHz. The results indicate that suppression of broadband interference by decorrelation varies from 4 to 34 dB, with strong dependence on the observing declination. The interference was assumed to extend uniformly across the bandwidth, which would tend to overestimate the suppression in a practical situation.

16.4 Very-Long-Baseline Systems

In VLBI arrays, in which the antenna spacings are hundreds or thousands of kilometers, the output resulting from correlated components of an interfering signal at the correlator inputs is usually negligible. This is because the natural fringe frequencies are higher than those in arrays with baselines up to a few tens of kilometers, and the delay inequalities for signals that do not come from the direction of observation are also much greater. Furthermore, unless the interfering signal originates in a satellite or spacecraft, it is unlikely to be present at two widely separated locations.

Consider an interfering signal entering one antenna of a correlated pair. The interference reduces the measured correlation, and the overall effect is similar to

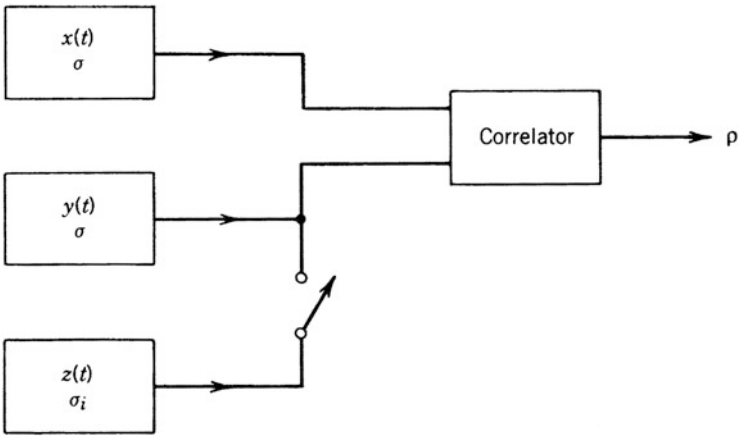

Fig. 16.4 Components of the correlator input signals used in the discussion of the effects of interference on VLBI observations.

an increase in the system noise for the antenna. In Fig. 16.4, $x(t)$ and $y(t)$ represent the signals plus system noise from two antennas in the absence of interference, and $z(t)$ represents an interfering signal at one antenna. The three waveforms have zero means, and the standard deviations are σ for x and y and σ_i for z. In the absence of interference, the measured correlation coefficient is

$$\rho_1 = \frac{\langle xy \rangle}{\sqrt{\langle x^2 \rangle \langle y^2 \rangle}} = \frac{\langle xy \rangle}{\sigma^2} \,. \tag{16.21}$$

When the interference is present, the correlation becomes

$$\rho_2 = \frac{\langle xy \rangle + \langle xz \rangle}{\sqrt{\langle x^2 \rangle \left(\langle y^2 \rangle + 2\langle yz \rangle + \langle z^2 \rangle \right)}} \,. \tag{16.22}$$

The interference is uncorrelated with x and y, so $\langle xz \rangle = \langle yz \rangle = 0$. Also, at the harmful threshold, $\sigma_i^2 \ll \sigma^2$. Thus, from Eqs. (16.21) and (16.22),

$$\rho_2 \simeq \rho_1 \left[1 - \frac{1}{2} \left(\frac{\sigma_i}{\sigma} \right)^2 \right] \,. \tag{16.23}$$

The interference reduces the measured correlation. In a system with automatic level control (ALC), the reduction in correlation can be envisaged as resulting from a reduction in the system gain in response to the added power of the interference. The error introduced in the correlation measurement therefore takes the form of a multiplicative factor, rather than an additive error component. Interference causes additive errors in single antennas or arrays that have short enough baselines that the detector or correlator responds directly to the interfering signal. The different

effects of these two types of error have been discussed in Sect. 10.6.3. In principle, the change in the effective gain can be monitored by using a calibration signal, as discussed in Sect. 7.6. However, such a calibration process could be difficult if the strength of the interference varies rapidly. The harmful interference threshold should therefore be specified so it is just small enough that the errors introduced do not significantly increase the level of uncertainty in the measurements. In general, a value of 1% for variations in the visibility amplitude resulting from interference is a reasonable choice. If we include the possibility of simultaneous but uncorrelated interference in both antennas, the resulting condition is

$$\left(\frac{\sigma_i}{\sigma}\right)^2 \leq 0.01 \; . \tag{16.24}$$

It follows from Parseval's theorem, that a 1% rms error in the visibility introduces into the intensity an error of which the rms over the image is 1% of the corresponding rms of the true intensity distribution. The effect on the dynamic range of intensity within the image depends on the form of the intensity distribution and of the error distribution. For an image of a single point source, the rms intensity error would be about $10^{-2}\sqrt{f/n_r}$ times the peak intensity, where f is the fraction of the n_r gridded visibility data that contain interference. Here it is assumed that the fluctuations in the received interfering signal are sufficiently fast that the values of the interference level are essentially independent for each gridded visibility point. If this is not the case, the resulting error will be greater.

To comply with the criterion in Eq. (16.24), the ratio of the powers of the interference to system noise as given by Eq. (16.2) must not exceed 0.01. Thus, for the harmful threshold, we have

$$F_h = \frac{0.04\pi k T_S \nu^2 \Delta\nu}{c^2} \; . \tag{16.25}$$

The interference threshold in units of W m^{-2} Hz^{-1} is

$$S_h = \frac{F_h}{\Delta\nu} = \frac{0.04\pi k T_S \nu^2}{c^2} \; . \tag{16.26}$$

Note that the interference-to-noise ratio of 0.01 here refers to the levels at the correlator input. In the case of total-power systems (single antennas) and the arrays considered in Sect. 16.3, for which the errors are additive, the criterion of an interference-to-noise ratio of 0.1 applies to the time-averaged output of the correlator or detector. This therefore results in lower (i.e., more stringent) thresholds than those for VLBI in Eqs. (16.25) and (16.26). A curve for VLBI is shown in Fig. 16.2, using typical values for T_S. The harmful thresholds are approximately 40–50 dB less stringent than those for total-power systems.

16.5 Interference from Airborne and Space Transmitters

In application of the F_h and S_h values obtained above, it was assumed that the angular distance between the pointing direction of the antenna beams and the direction of the source of interference is large enough that the interference enters through sidelobes of gain $\sim$ 1 dB or less, i.e., that the angular distance is $\sim$ 19° or more. Thus, airborne and satellite transmitters present a special problem. Radio astronomy cannot share bands with space-to-Earth (downlink) transmissions of satellites. However, because of the pressure for more spectrum for communications, allocations have been made in bands adjacent or close to those allocated to radio astronomy. Spurious emissions from satellite transmitters that fall outside the allocated band of the satellite pose a very serious threat to radio astronomy. Motion of the transmitter across the sky is most likely to increase the fringe frequency at the correlator outputs of a synthesis array and thereby reduce the response to interference. On the other hand, these signals may be received in high-level sidelobes near the main beam.

Examples of spurious emissions that extend far outside the allocated band of the satellite system are described by Galt (1990) and Combrinck et al. (1994). In these cases, the spurious emission resulted largely from the use of simple phase shift keying for the modulation, and newer techniques (e.g., Gaussian-filtered minimum shift keying) provide much sharper reduction in spectral sidebands (Murota and Hirade 1981; Otter 1994). However, intermodulation products resulting from the nonlinearity of amplifiers carrying many communication channels can remain a problem.

In some cases, operating requirements and limitations associated with space tend to make reduction of spurious emissions difficult. Some satellites use a large number of narrow beams to cover their area of operation, so that the same frequency channels can be used a corresponding number of times to accommodate a large number of customers. This requires phased-array antennas with many (of order 100 or more) small radiating elements, each with its own power amplifier [see, e.g., Schuss et al. (1999)]. Because of power limitations from the solar cells, these amplifiers are operated at levels that maximize power efficiency but could compromise linearity, resulting in spurious emissions from intermodulation products.

The recommended limits on spurious emissions (ITU-R 2012) in effect require that, for space services, the power in spurious emissions measured in a 4-kHz band at the transmitter output should be no more than –43 dBW. Thus, for example, spurious emission at this level from a low-Earth-orbit satellite at 800 km height and radiated from a sidelobe of 0 dBi gain would produce a spurious spectral power flux density of –208 dBW m^{-2} Hz^{-1} at the Earth's surface. This figure may be compared with the harmful interference thresholds for radio astronomy of –239 and –255 dBW m^{-2} Hz^{-1} for spectral line and continuum measurements, respectively, at 1.4 GHz. Although this very simple calculation considers only the worst-case situation, the differences of several tens of decibels show that such limits do not effectively protect radio astronomy.

16.6 Regulation of the Radio Spectrum

Regulation of the usage of the radio spectrum is organized through ITU, based in Geneva, which is a specialized agency of the United Nations. Radio astronomy was first officially recognized as a radiocommunication service by the ITU in 1959. The ITU-R was created in March 1993 and replaced the International Radio Consultative Committee (CCIR), an earlier entity within the ITU. A system of study groups within the ITU-R is responsible for technical matters. Study Group 7, entitled Science Services, includes radio astronomy, various aspects of space research, environmental monitoring, and standards for time and frequency. Study groups are subdivided into working parties that deal with specific areas. Their primary function is to study problems of current importance in frequency coordination, for example, specific cases of sharing of frequency bands between different services, and to produce documented Recommendations on the solutions. Decisions within the ITU are made largely by consensus. Recommendations must be approved by all of the radiocommunication study groups and then effectively become part of the ITU Radio Regulations. Recommendations in the RA series are specific to radio astronomy.

The ITU-R organizes meetings of study groups, working parties, and other groups required from time to time to deal with specific problems. It also organizes World Radiocommunication Conferences (WRCs) at intervals of two to three years, at which new spectrum allocations are made and the ITU Radio Regulations are revised as necessary. Administrations of many countries send delegations to WRCs, and the results of these conferences have the status of treaties. Participating countries can take exceptions to the international regulations so long as these do not affect spectrum usage in other countries. As a result, many administrations have their own system of radio regulations, based largely on the ITU Radio Regulations but with exceptions to accommodate their particular requirements: see Pankonin and Price (1981) and Thompson et al. (1991). See also ITU-R *Handbook on Radio Astronomy* (2013) and ITU-R Recommendation RA.769-2 (2003).

Further Reading

Crawford, D.L., Ed., *Light Pollution, Radio Interference, and Space Debris*, Astron. Soc. Pacific Conf. Ser., **17** (1991)

Ellingson, S., Introduction to Special Section on Mitigation of Radio Frequency Interference in Radio Astronomy, *Radio Sci.*, **40**, No. 5 (2005) (*Radio Sci.*, **40**, No. 5, contains 17 articles of interest.)

ITU-R, *Handbook on Radio Astronomy*, International Telecommunication Union, Geneva (2013)

Kahlmann, H.C., Interference: The Limits of Radio Astronomy, in *Review of Radio Science 1996–1999*, Stone, W.R., Ed., Oxford Univ. Press, Oxford, UK (1999), pp. 751–785

National Research Council, *Handbook of Frequency Allocations and Spectrum Protection for Scientific Uses,* 2nd ed., National Academies Press, Washington, DC (2015)

National Research Council, *Spectrum Management for Science in the 21st Century*, National Academies Press, Washington, DC (2010)

Swenson, G.W., Jr., and Thompson, A.R., Radio Noise and Interference, in *Reference Data for Engineers: Radio, Electronics, Computer, and Communications*, 8th ed., Sams, Indianapolis, IN (1993)

References

Athreya, R., A New Approach to Mitigation of Radio Frequency Interference in Interferometric Data, *Astrophys. J.*, **696**, 885–890 (2009)

Baan, W.A., RFI Mitigation in Radio Astronomy, in *Proc. of RFI Mitigation Workshop*, Proc. Science, PoS(RFI2010)011 (2010)

Barnbaum, C., and Bradley, R.F., A New Approach to Interference Excision in Radio Astronomy: Real-Time Adaptive Cancellation, *Astron. J.*, **116**, 2598–2614 (1998)

Beasley, W.L., "An Investigation of the Radiated Signals Produced by Small Sparks on Power Lines," Ph.D. thesis, Texas A&M Univ. (1970)

Bhat, N.D.R., Cordes, J.M., Chatterjee, S., and Lazio, T.J.W., Radio Frequency Interference Identification and Mitigation, Using Simultaneous Dual-Station Observations, *Radio Sci.*, **40**, RS5S14 (2005)

Boonstra, A.J., and van der Tol, S., Spatial Filtering of Interfering Signals at the Initial Low-Frequency Array (LOFAR) Phased Array Test Station, *Radio Sci.*, **40**, RS5S09 (2005)

Bretteil, S., and Weber, R., Comparison of Two Cyclostationary Detectors for Radio Frequency Interference Mitigation in Radio Astronomy, *Radio Sci.*, **40**, RS5S15 (2005)

Briggs, F.H., Bell, J.F., and Kesteven, M.J., Removing Radio Interference from Contaminated Astronomical Spectra Using an Independent Reference Signal and Closure Relations, *Astron. J.*, **120**, 3351–3361 (2000)

Briggs, F.H., and Kocz, J., Overview of Approaches to Radio Frequency Interference Mitigation, *Radio Sci.*, **40**, RS5S02 (2005)

Combrinck, W.L., West, M.E., and Gaylord, M.J., Coexisting with GLONASS: Observing the 1612-MHz Hydroxyl Line, *Publ. Astron. Soc. Pacific*, **106**, 807–812 (1994)

Dong, W., Jeffs., B.D., and Fisher, J.R., Radar Interference Blanking in Radio Astronomy Using a Kalman Tracker, *Radio Sci.*, **40**, RS5S04 (2005)

Ellingson, S.W., Bunton, J.D., and Bell, J.F., Removal of the GLONASS C/A Signal from OH Spectral Line Observations Using a Parametric Modeling Technique, *Astron. J. Suppl.*, **135**, 87–93 (2001)

Ellingson, S.W., and Cazemier, W., Efficient Multibeam Synthesis with Interference Nulling for Large Arrays, *IEEE Trans. Antennas Propag.*, **51**, 503–511 (2003)

Ellingson, S.W., and Hampson, G.A., A Subspace Tracking Approach to Interference Nulling for Phased Array Based Radio Telescopes, *IEEE Trans. Antennas Propag.*, **50**, 25–30 (2002)

Fridman, P.A., and Baan, W.A., RFI Mitigation in Radio Astronomy, *Astron. Astrophys.*, **378**, 327–344 (2001)

Galt, J., Contamination from Satellites, *Nature*, **345**, 483 (1990)

ITU-R, *Handbook on Radio Astronomy*, International Telecommunication Union, Geneva (2013)

ITU-R Recommendation SA.509-1, Generalized Space Research Earth Station Antenna Radiation Pattern for Use in Interference Calculations, Including Coordination Procedures, *ITU-R Recommendations, SA Series*, International Telecommunication Union, Geneva (1997) (see also updated Recommendation SA.509-3, 2013)

ITU-R Recommendation RA.769-2, Protection Criteria Used for Radio Astronomical Measurements, *ITU-R Recommendations, RA Series*, International Telecommunication Union, Geneva (2003) (or current revision)

ITU-R Recommendation SM.329-12, Unwanted Emissions in the Spurious Domain, *ITU-R Recommendations, SA Series*, International Telcommunication Union, Geneva (2012) (or current revision)

Leshem, A., and van der Veen, A.-J., Radio-Astronomical Imaging in the Presence of Strong Radio Interference, *IEEE Trans. Inform. Theory*, **46**, 1730–1747 (2000)

Leshem, A., van der Veen, A.-J., and Boonstra, A.-J., Multichannel Interference Mitigation Techniques in Radio Astronomy, *Astrophys. J. Suppl.*, **131**, 355–373 (2000)

Murota, K., and Hirade, K., GMSK Modulation for Digital Mobile Radio Telephony, *IEEE Trans. Commun.*, **COM-29**, 1044–1050 (1981)

Nita, G.M., and Gary, D.E., Statistics of the Spectral Kurtosis Estimator, *Publ. Astron. Soc. Pacific*, **122**, 595–607 (2010)

Nita, G.M., Gary, D.E., Lui, Z., Hurford, G.H., and White, S.M., Radio Frequency Interference Excision Using Spectral Domain Statistics, *Publ. Astron. Soc. Pacific*, **119**, 805–827 (2007)

Offringa, A.R., de Bruyn, A.G., Zaroubi, S., van Diepen, G., Martinez-Ruby, O., Labropoulos, P., Brentjens, M.A., Ciardi, B., Daiboo, S., Harker, G., and 86 coauthors, The LOFAR Radio Environment, *Astron. Astrophys.*, **549**, A11 (15pp) (2013)

Offringa, A.R., Wayth, R.B., Hurley-Walker, N., Kaplan, D.L., Barry, N., Beardsley, A.P., Bell, M.E., Bernardi, G., Bowman, J.D., Briggs, F., and 55 coauthors, The Low-Frequency Environment of the Murchison Widefield Array: Radio-Frequency Interference Analysis and Mitigation, *Publ. Astron. Soc. Aust.*, **32**, e008 (13pp) (2015)

Otter, M., A *Comparison of QPSK, OQPSK, BPSK, and GMSK Modulation Schemes*, Report of the European Space Agency, European Space Operations Center, Darmstadt, Germany (1994)

Pankonin, V., and Price, R.M., Radio Astronomy and Spectrum Management: The Impact of WARC-79, *IEEE Trans. Electromag. Compat.*, **EMC-23**, 308–317 (1981)

Perley, R., Attenuation of Radio Frequency Interference by Interferometric Fringe Rotation, EVLA Memo 49, National Radio Astronomy Observatory (2002)

Petroff, E., Keane, E.F., Barr, E.D., Reynolds, J.E., Sarkissian, J., Edwards, P.G., Stevens, J., Brem, C., Jameson, A., Burke-Spolaor, S., and four coauthors, Identifying the Source of Perytons at the Parkes Radio Telescope, *Mon. Not. R. Astron. Soc.*, **451**, 3933–3940 (2015)

Raza, J., Boonstra, A.-J., and van der Veen, A.-J., Spatial Filtering of RF Interference in Radio Astronomy, *IEEE Signal Proc. Lett.*, **9**, 64–67 (2002)

Rogers, A.E.E., Pratap, P., Carter, J.C., and Diaz, M.A., Radio Frequency Interference Shielding and Mitigation Techniques for a Sensitive Search for the 327-MHz Line of Deuterium, *Radio Sci.*, **40**, RS5S17 (2005)

Schuss, J.J., Upton, J., Myers, B., Sikina, T., Rohwer, A., Makridakas, P., Francois, R., Wardle, L., and Smith, R., The IRIDIUM Main Mission Antenna Concept, *IEEE Trans. Antennas Propag.*, **AP-47**, 416–424 (1999)

Smolders, B., and Hampson, G., Deterministic RF Nulling in Phased Arrays for the Next Generation of Radio Telescopes, *IEEE Antennas Propag. Mag.*, **44**, 13–22 (2002)

Thompson, A.R., The Response of a Radio-Astronomy Synthesis Array to Interfering Signals, *IEEE Trans. Antennas Propag.*, **AP-30**, 450–456 (1982)

Thompson, A.R., Gergely, T.E., and Vanden Bout, P., Interference and Radioastronomy, *Physics Today*, **44**, 41–49 (1991)

van der Tol, S., and van der Veen, A.-J., Performance Analysis of Spatial Filtering of RF Interference in Radio Astronomy, *IEEE Trans. Signal Proc.*, **53**, 896–910 (2005)